raises the question whether the weak feature seen at 16 500 cm^{-1} in a single-crystal study of $Re_2(piv)_4Cl_2$[7] was due to the presence of very small amounts of the rearranged form. Similar weak, low-energy bands have been observed in the solution spectra of several dirhenium tetracarboxylate bromides and iodides.[25]

In summary, the changes seen in the visible and infrared spectra for $Re_2(piv)_4Cl_2$ and $Re_2(piv)_4Br_2$, both in the polycrystalline state and in a polymer matrix, indicate that pressure induces a molecular transformation leading to radial halide ligands and two monodentate pivalate ligands.

Acknowledgment. This work was supported in part by the Materials Science Division of the Department of Energy under Contract DE-AC02-76Er01198 and in part by the Division of Materials Research of the National Science Foundation under Grant DMR 86-12860. We acknowledge helpful comments from Dr. Basil Swanson in arriving at the interpretation of our results.

(25) Srinivasan, V.; Walton, R. A. *Inorg. Chem.* **1980**, *19*, 1635.

Contribution from the Department of Chemistry,
Texas A&M University, College Station, Texas 77843

Determination of Magnetic and Structural Properties in Solids Containing Antiferromagnetically Coupled Metal Centers Using NMR Methods. Magneto-Structural Correlations in Anhydrous Copper(II) *n*-Butyrate

Gordon C. Campbell and James F. Haw*

Received March 18, 1988

A new approach to the investigation of magneto-structural correlations in solids containing antiferromagnetically coupled transition-metal centers is described that illustrates the potential of NMR spectroscopy in such work. In this contribution we report the results of a variable-temperature (VT) ^{13}C cross-polarization magic-angle-spinning (CP/MAS) NMR investigation of anhydrous copper(II) *n*-butyrate, $[Cu(C_3H_7COO)_2]_2$. Isotropic shifts are found to be primarily contact in origin, and a statistical analysis of their temperature dependence allows the calculation of singlet-triplet energy level separations ($-2J$), diamagnetic shifts (δ_{dia}), and electron-nucleus hyperfine coupling constants (A), which are shown to give insight into the mechanisms of electron delocalization along the superexchange pathway. Signal multiplicity can be related to compound structure, which was determined by using X-ray crystallography. The title compound is triclinic and has a space group of $P\bar{1}$ with a = 9.035 (2) Å, b = 5.192 (2) Å, c = 11.695 (3) Å, α = 85.88 (2)°, β = 95.04 (2)°, γ = 109.32 (2)°, Z = 1, and V = 515.2 (3) Å^3; the final weighted R value for 2169 reflections was 0.048.

Introduction

Solid copper(II) carboxylates, $Cu_2(RCO_2)_4L_n$ with n = 0 or n = 2, are prototypical examples of transition-metal complexes that contain two or more antiferromagnetically coupled metal centers.[1] Much emphasis has been placed on the development of magneto-structural correlations in these systems,[2] as reflected by the description of magnetic coupling between Cu(II) centers that appears in the literature. Originally thought to be the result of direct Cu-Cu bonding, either δ[3] or σ,[4] the antiferromagnetic interaction is now recognized to be propagated through the electronic orbitals of ligands bridging the metal centers in what is termed the superexchange pathway.[5] Much current research is directed toward the development of a more complete understanding of magnetic superexchange, but achievement of this goal has been hampered (in part) by the limited number of spectroscopic methods amenable to solid transition-metal complexes.

Recently, though, the potential of solid-state NMR methods has been demonstrated by preliminary variable-temperature studies of copper(II) carboxylates that revealed temperature-dependent chemical shifts and line widths.[6] Up until now these results have been primarily qualitative in nature. We demonstrate here that suitable solid-state NMR experiments can effectively probe the superexchange pathway and allow the quantitative measurement of electron-nucleus hyperfine coupling constants, structurally significant chemical shifts, and singlet-triplet energy level separations for a representative member of this class. This is a natural extension of some of our previous work on the cross-polarization magic-angle-spinning (CP/MAS) NMR of paramagnetic solids.[7]

Experimental Section

Compound Preparation and NMR Methods. Anhydrous copper(II) *n*-butyrate, $Cu_2(C_3H_7CO_2)_4$, was prepared by using standard literature methods[8] and packed into a Kel-F NMR rotor. Spectroscopic studies were carried out on approximately 0.3 g of powder. All variable-temperature[9] ^{13}C CP/MAS NMR spectra were obtained at 25.02 MHz on a Chemagnetics M-100S spectrometer with a 1-ms cross-polarization contact time and a repetition delay of 1 s. Magic-angle-spinning rates used typically ranged between 4 kHz at ambient temperatures and 2.5 kHz at cryogenic temperatures. A total of 400 transients were collected at each temperature and multiplied by an exponential weighting function of 50 Hz before transforming. Spectral assignments were facilitated by the interrupted decoupling experiment.[10] Statistical analyses of tem-

Table I. Crystallographic Data for Anhydrous Copper(II) *n*-Butyrate

chem formula	fw 475.5
$C_{16}H_{28}O_8Cu_2$	space group $P\bar{1}$
a = 9.035 (2) Å	T = 20 °C
b = 5.192 (2) Å	λ = 0.7107 Å
c = 11.695 (3) Å	ρ_{obsd} = 1.55 g cm^{-3}, ρ_{calcd} = 1.53 g cm^{-3}
α = 85.88 (2)°	μ = 21.1 cm^{-1}
β = 95.04 (2)°	rel transmission factors 0.464-1.000
γ = 109.32 (2)°	$R(F_o^2)$ = 0.039
V = 515.2 (3) Å^3	$R_w(F_o^2)$ = 0.048
Z = 1	

* To whom correspondence should be addressed.

(1) (a) Jotham, R. W.; Kettle, S. F. A.; Marks, J. A. *J. Chem. Soc., Dalton Trans.* **1972**, 428. (b) Melnik, M. *Coord. Chem. Rev.* **1982**, *42*, 259. (c) Folgado, J. V.; Ibanez, R.; Coronado, E.; Beltran, D.; Savariault, J. M.; Galy, J. *Inorg. Chem.* **1988**, *27*, 19. (d) Thompson, L. K.; Lee, F. L.; Gabe, E. J. *Inorg. Chem.* **1988**, *27*, 39.
(2) Willett, R. D., Gatteschi, D., Kahn, O., Eds. *Magneto-Structural Correlations in Exchange Coupled Systems*; Reidel: Boston, MA, 1985.
(3) Figgis, B. N.; Martin, R. L. *J. Chem. Soc.* **1956**, 3837.
(4) Forster, L. S.; Ballhausen, C. J. *Acta Chem. Scand.* **1962**, *16*, 1385.
(5) Gerloch, M.; Harding, J. H. *Proc. R. Soc. London, A* **1978**, *360*, 211.
(6) (a) Haw, J. F. Presentation at the 28th Rocky Mountain Conference, Denver, CO, 1986. (b) Campbell, G. C. Presentation at the 28th Experimental NMR Conference, Asilomar, CA, 1987. (c) Campbell, G. C. Presentation at the 29th Rocky Mountain Conference, Denver, CO, 1987. (d) Walter, T. H.; Oldfield, E. *J. Chem. Soc., Chem. Commun.* **1987**, 646.
(7) (a) Haw, J. F.; Campbell, G. C. *J. Magn. Reson.* **1986**, *66*, 558. (b) Campbell, G. C.; Crosby, R. C.; Haw, J. F. *J. Magn. Reson.* **1986**, *69*, 191.
(8) Martin, R. L.; Waterman, H. *J. Chem. Soc.* **1957**, 2545.
(9) Haw, J. F.; Campbell, G. C.; Crosby, R. C. *Anal. Chem.* **1986**, *58*, 3172.

0020-1669/88/1327-3706$01.50/0 © 1988 American Chemical Society

Table II. Atomic Coordinates (×10⁴) and Equivalent Isotropic Displacement Parameters (Å² × 10³)[a]

atom	x	y	z	U(eq)
Cu	5230 (1)	2353 (1)	4466 (1)	29 (1)
O(1)	4552 (2)	3289 (4)	5929 (2)	32 (1)
O(2)	4171 (3)	−767 (4)	6825 (2)	44 (1)
C(1)	4169 (3)	1652 (5)	6789 (3)	32 (1)
C(2)	3658 (5)	2674 (7)	7799 (3)	52 (1)
C(3)	3392 (8)	975 (10)	8842 (4)	92 (3)
C(4)	2818 (7)	2039 (12)	9790 (4)	96 (3)
O(3)	3055 (3)	882 (4)	3888 (2)	47 (1)
O(4)	2646 (2)	−3154 (4)	4828 (2)	44 (1)
C(5)	2217 (3)	−1520 (6)	4164 (3)	39 (1)
C(6)	545 (4)	−2522 (7)	3626 (4)	51 (1)
C(7)	181 (5)	−5173 (8)	3023 (4)	57 (1)
C(8)	1136 (7)	−4871 (13)	2007 (5)	92 (3)

[a] Equivalent isotropic U defined as one-third of the trace of the orthogonalized U_{ij} tensor.

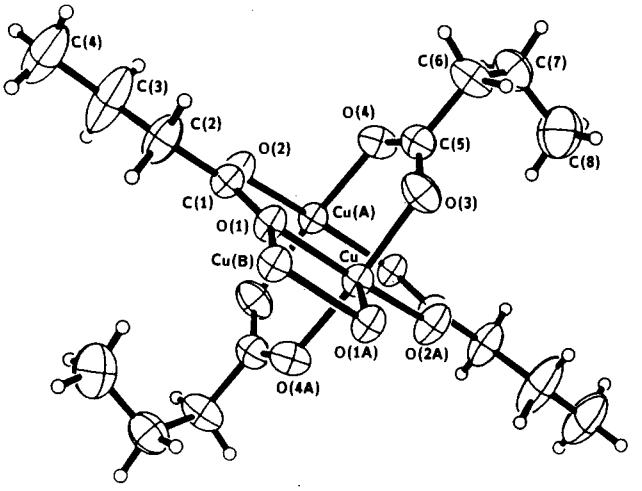

Figure 1. ORTEP projection of anhydrous copper(II) *n*-butyrate, $[Cu(C_3H_7COO)_2]_2$, showing 50% thermal ellipsoids and atom-labeling scheme. Atoms Cu(A), Cu(B), O(1A), O(2A), and O(4A) are generated by an inversion operation.

perature-dependent chemical shift data were done with the NLIN program of the SAS (Statistical Analysis Service) package.

Crystallographic Data Collection and Structure Determination. Single crystals of $[Cu(C_3H_7COO)_2]_2$ were grown from butyric acid solution and sent to the Crystalytics Co. (Lincoln, NE) for crystallographic data collection, the details of which are summarized in Table I. A more complete report on the structure solution is included as supplementary material (Table SI). A blue-green rectangular parallelepiped crystal was mounted in a glass capillary for intensity data collection on a Nicolet P1 diffractometer. Data were worked up by routine procedures, an empirical absorption correction (ψ scan) was applied, and the structure was solved by direct methods using the SHELXTL-Plus program library[11] at Texas A&M University. The combination of intensity statistics with solid-state NMR data (vide infra) allowed unambiguous space group ($P\bar{1}$) determination. Extinction corrections were not done, and H atom positions were calculated. Final atomic positional parameters and equivalent isotropic displacement parameters are given in Table II. The structure of anhydrous copper(II) *n*-butyrate is presented in Figure 1, with bond distances and angles given in Table III. Anisotropic thermal parameters (Table SII), calculated H atom coordinates (Table SIII), and a listing of structure factors are available as supplementary material.

Results and Discussion

^{13}C CP/MAS NMR spectra representative of those obtained at 19 temperatures between 298 K and 77 K are presented in Figure 2. The numbering system used to describe the NMR assignments is identical with that used in the ORTEP projection (Figure 1). For example, C(4) and C(8) refer to methyl carbon resonances on the two crystallographically inequivalent alkyl chains. The solid-state NMR spectra are characterized by temperature-dependent chemical shifts and line widths that, below the critical temperature, increase in magnitude with increasing temperature and (to a first approximation) decreasing distance from the metal centers. The critical temperature, T_C, is defined as the temperature above which the susceptibility of these materials decreases as T increases (T_C = 290 K for the title compound[8]). Inspecting Figure 2, one notes the presence of two magnetically inequivalent methyl carbon resonances (C(4) and C(8)). The rationale for assigning the C(4) and C(8) resonances to specific crystallographic sites will be justified later in this contribution.

Table III. Bond Lengths (Å) and Angles (deg) in $[Cu(C_3H_7COO)_2]_2$

Cu–O(1)	2.010 (2)	Cu–O(3)	1.936 (2)
Cu–Cu(A)	2.584 (1)	Cu–O(1A)	2.223 (2)
Cu–O(2A)	1.966 (3)	Cu–O(4A)	1.944 (2)
O(1)–C(1)	1.263 (3)	O(1)–Cu(B)	2.223 (2)
O(2)–C(1)	1.254 (4)	O(2)–Cu(A)	1.966 (3)
C(1)–C(2)	1.496 (5)	C(2)–C(3)	1.443 (6)
C(3)–C(4)	1.476 (9)	O(3)–C(5)	1.262 (3)
O(4)–C(5)	1.242 (4)	O(4)–Cu(A)	1.944 (2)
C(5)–C(6)	1.519 (4)	C(6)–C(7)	1.516 (6)
C(7)–C(8)	1.498 (8)		

O(1)–Cu–O(3)	90.3 (1)	O(1)–Cu–Cu(A)	82.8 (1)
O(3)–Cu–Cu(A)	85.6 (1)	O(1)–Cu–O(1A)	79.4 (1)
O(3)–Cu–O(1A)	95.8 (1)	Cu(A)–Cu–O(1A)	162.2 (1)
O(1)–Cu–O(2A)	169.4 (1)	O(3)–Cu–O(2A)	88.8 (1)
Cu(A)–Cu–O(2A)	86.6 (1)	O(1A)–Cu–O(2A)	111.2 (1)
O(1)–Cu–O(4A)	89.3 (1)	O(3)–Cu–O(4A)	169.4 (1)
Cu(A)–Cu–O(4A)	83.9 (1)	O(1A)–Cu–O(4A)	94.5 (1)
O(2A)–Cu–O(4A)	89.7 (1)	Cu–O(1)–C(1)	124.5 (2)
Cu–O(1)–Cu(B)	100.6 (1)	C(1)–O(1)–Cu(B)	134.9 (2)
C(1)–O(2)–Cu(A)	122.6 (2)	O(1)–C(1)–O(2)	123.5 (3)
O(1)–C(1)–C(2)	117.4 (3)	O(2)–C(1)–C(2)	119.1 (3)
C(1)–C(2)–C(3)	118.8 (4)	C(2)–C(3)–C(4)	116.2 (5)
Cu–O(3)–C(5)	121.4 (2)	C(5)–O(4)–Cu(A)	123.4 (2)
O(3)–C(5)–O(4)	125.7 (3)	O(3)–C(5)–C(6)	117.4 (3)
O(4)–C(5)–C(6)	117.0 (2)	C(5)–C(6)–C(7)	112.7 (3)
C(6)–C(7)–C(8)	112.7 (3)		

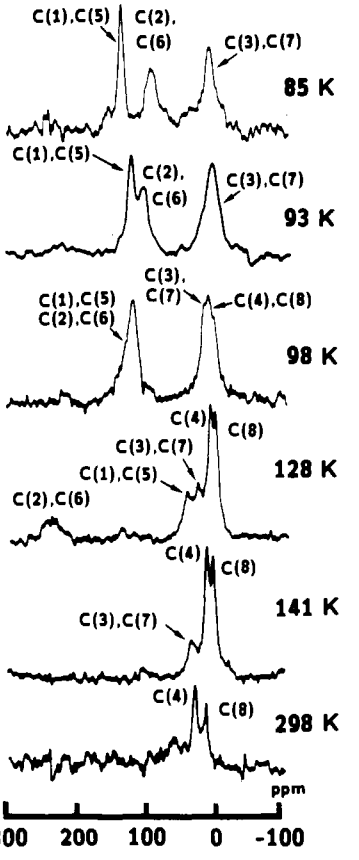

Figure 2. Variable-temperature ^{13}C CP/MAS NMR spectra of anhydrous copper(II) *n*-butyrate. Signal assignments are based on the numbering scheme established in Figure 1.

(10) Opella, S. J.; Frey, M. H. *J. Am. Chem. Soc.* **1979**, *101*, 5854.
(11) G. M. Sheldrick; supplied by Nicolet XRD.

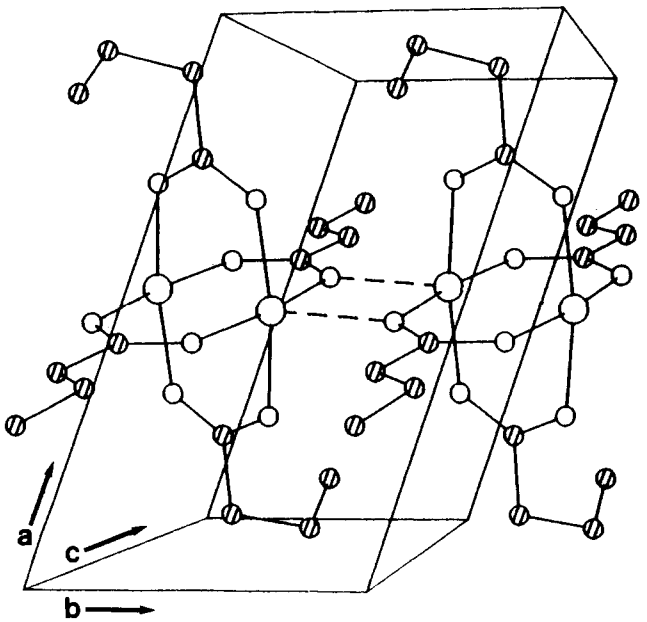

Figure 3. Unit cell of anhydrous copper(II) *n*-butyrate including two dimeric repeat units.

Similar, but less pronounced, magnetic inequivalencies are sometimes observed in solid-state NMR spectra of diamagnetic compounds due to nuclear occupation of crystallographically distinct sites in the unit cell.

The crystal structure of copper(II) *n*-butyrate has appeared in the literature,[12] but the reported *R* value (0.092) motivated a redetermination. Our measurement yielded the structure shown in Figure 1 and described by the parameters presented in Tables II and III. Pairs of copper ions separated by 2.58 Å are bridged by four *n*-butyrate ligands to give a dimeric structure analogous to that known for copper(II) acetate hydrate. Instead of water molecules at axial coordination sites, oxygen atoms from adjacent dimeric units complete the copper coordination in this anhydrous material. The resulting structure consists of chains of copper(II) *n*-butyrate dimers. Figure 3 is a drawing of the unit cell, which shows that there are two inequivalent types of carboxylate ligands. The inequivalence is most pronounced for the two sets of methyl carbons and is reflected in the NMR spectra. Relatively broad NMR line widths for the resonances due to carbons closer to the metal centers, combined with less inequivalent positions in the unit cell, prevent us from observing the expected multiplicities for those signals. Methyl resonances are not observed at temperatures between 93 and 77 K due to methyl group motion on the order of the decoupler frequency (γB_1 = 48 kHz).[13]

Figure 4 is a representative plot of chemical shift versus temperature for one of the resonances, C(4). ×'s indicate experimental points, and the solid curve is the theoretical fit. Analogous plots were obtained for the other ^{13}C resonances (not shown). This variation of chemical shift with temperature for the ^{13}C resonances of copper(II) *n*-butyrate is very similar in form to that seen for the variation of magnetic susceptibility with temperature in copper(II) carboxylates.[8] Both magnetic parameters increase with temperature up to T_C; beyond this they decrease due to thermal randomization of the unpaired electron orientation.

It is this temperature dependence of the chemical shifts that allows the calculation of hyperfine coupling constants (A), apparent singlet state–triplet state energy level splittings ($-2J$, from the spin Hamiltonian $H = -2J\hat{S}_1\cdot\hat{S}_2$), and diamagnetic chemical shifts (δ_{dia}) for each resolved carbon site. Beginning with basic theories of magnetism[14] and NMR of paramagnetic materials[15]

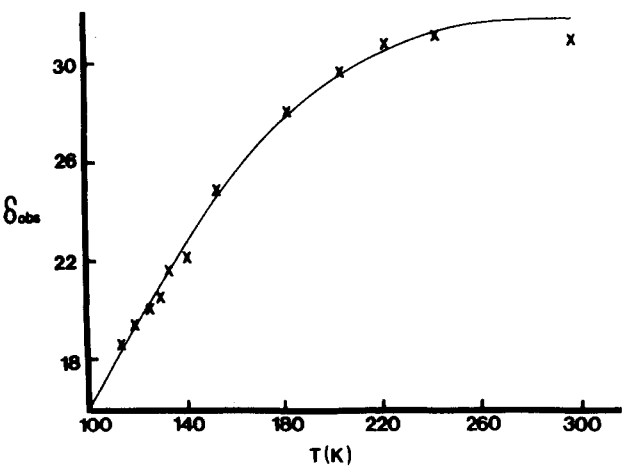

Figure 4. Plot of C(4) chemical shift vs absolute temperature for the title compound. ×'s are experimental points, and the solid curve is the theoretical fit. Analogous plots were obtained for all other ^{13}C resonances except that of C(8) (see text).

Table IV. Calculated Magnetic and Electronic Parameters for Anhydrous Copper(II) *n*-Butyrate[a]

	carbon			
	C(1), C(5)	C(2), C(6)	C(3), C(7)	C(4)
$-2J$, cm^{-1}	−288 ± 12	−312 ± 8	−317 ± 3	−322 ± 6
A, MHz[b]	−1.90 ± 0.3	3.96 ± 0.4	0.432 ± 0.009	0.168 ± 0.003
A, MHz[c]	−2.74 ± 0.07	4.61 ± 0	0.474 ± 0.006	0.181 ± 0.003
$\delta_{dia,calc}$	188 ± 7	43 ± 8	17 ± 0.7	12 ± 0.8
$\delta_{dia,expt}$[d]	183	40	21	14

[a] Uncertainties are expressed as one standard deviation. [b] From a three-parameter fit. [c] From a two-parameter fit with $-2J$ constrained to −322 cm^{-1}.[8] [d] ^{13}C chemical shifts of sodium *n*-butyrate, a diamagnetic model compound. All chemical shifts are in ppm.

and assuming a contact-shift model, one can derive the following equation to describe the variation of the NMR chemical shifts with temperature in magnetically coupled d^9–d^9 systems:[16]

$$H_{obs} = H_{dia} + \frac{2g\beta H_0 A}{(\gamma_C/2\pi)kT}(3 + e^{2J/kT})^{-1} \qquad (1)$$

where H_{obs} is the frequency of the ^{13}C resonance, H_{dia} is the frequency that the same nucleus would have in an equivalent diamagnetic environment, T is the absolute temperature, and the other terms have their usual meanings. Equation 1 will accurately describe the temperature dependence of the chemical shifts only if the dipolar contribution to the observed shifts is negligible. Metal-centered dipolar contributions to the paramagnetic shifts (ΔH^M) were thus estimated by using the reported g value anisotropy of the title compound,[17] the crystallographic data (Table III), and the theory developed by Kurland and McGarvey[15] modified to account for the distribution of electronic spins between the $S = 0$ and $S = 1$ states:

$$\frac{\Delta H^M}{H_0} = \frac{2\beta^2}{3kTR^3}(g_\parallel^2 - g_\perp^2)(1 - 3\cos^2\omega)(3 + e^{2J/kT})^{-1} \qquad (2)$$

ω is the angle between the electron–nucleus vector and the tetragonal axis of the complex, and R is the electron–nucleus distance. The metal-centered dipolar shifts estimated by using eq 2 were too small to account for the magnitude of the observed shifts, and were ignored.

$-2J$, H_{dia}, and A values were calculated by using a multiple-parameter, nonlinear least-squares procedure to fit the variable-temperature CP/MAS NMR data to eq 1. C(8) resonances could

(12) Bird, M. J.; Lomer, T. R. *Acta Crystallogr., Sect. B* **1972**, *28*, 242.
(13) Rothwell, W. P.; Waugh, J. S. *J. Chem. Phys.* **1981**, *74*, 2721.
(14) Carlin, R. E. *Magnetochemistry*; Springer-Verlag: New York, 1986; Chapter 2.
(15) Kurland, R. J.; McGarvey, B. R. *J. Magn. Reson.* **1970**, *2*, 286.
(16) (a) Boersma, A. D.; Phillippi, M. A.; Goff, H. M. *J. Magn. Reson.* **1984**, *57*, 197. (b) Holm, R. H.; Hawkins, C. J. In *NMR of Paramagnetic Molecules*; La Mar, G. N., Horrocks, W. DeW., Holm, R. H., Eds.; Academic: New York, 1973; Chapter 7.
(17) Battaglia, L. P.; Corradi, A. B.; Menabue, L. *J. Chem. Soc., Dalton Trans.* **1986**, 1653.

not be reliably fit to the model as they varied only ~1.5 ppm over the entire temperature range in which they were observable, indicating a very small hyperfine coupling constant for this site (vide infra). Calculated parameters for C(1) through C(7) are reported in Table IV along with uncertainties that represent one standard deviation. $-2J$ values (Table IV) agree quite well with the literature value of -322 cm^{-1} obtained from bulk magnetic susceptibility measurements,[8] especially for carbons further removed from the metal centers, for which we have chemical shift data over a wider temperature range and greater confidence in the contact-shift model. It is worthwhile to point out that since NMR methods probe local magnetic effects, solid-state NMR determinations of $-2J$ are not sensitive to traces of paramagnetic impurities as are bulk susceptibility measurements. Diamagnetic shifts calculated for the title compound are comparable to those that we measured in the solid state for a diamagnetic model compound, sodium *n*-butyrate (Table IV). This observation gives us additional confidence in the reliability of the fitting procedures and suggests the possibility of future correlations between chemical shift and structure.

Electron–nucleus hyperfine coupling constants (A values) were used to provide insight into the mechanisms of electron delocalization along the superexchange pathway and, in conjunction with the crystal structure, to assign C(4) and C(8) resonances. These A values were determined in two ways: from a three-parameter fit of the temperature dependence of the ^{13}C CP/MAS NMR chemical shifts and through a separate two-parameter fit with $-2J$ fixed to the literature value[8] of -322 cm^{-1}. This latter procedure allows a more reliable determination of the electron–nucleus hyperfine coupling constant, since it involves fewer unconstrained parameters.

Methyl carbon signals (C(4) and C(8)) were assigned to specific crystallographic sites on the basis of the relative magnitudes of their A values. In a manner analogous to that used for torsional-angle dependence on $^3J_{C-H}$[18a] and $^3J_{C-C}$[18b] values, electron–nucleus hyperfine coupling constants can be related to the dihedral angle between the orbital containing the unpaired electron density and the carbon nucleus of interest.[19] Newman projections

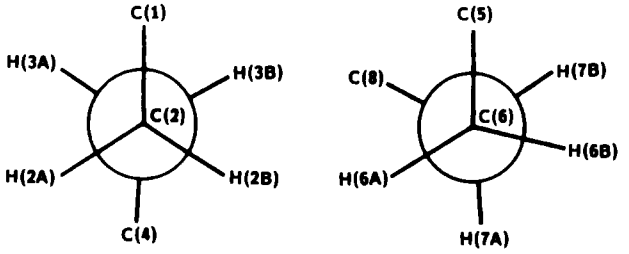

drawn on the basis of our structural determination illustrate the pronounced angular differences between crystallographically inequivalent carboxylate bridges. If it is assumed that net electron spin is associated primarily with the bond between C(1) and C(2) (or C(5) and C(6)), the relevant dihedral angles are $\theta_{C(1)-C(4)}$ (177°) and $\theta_{C(5)-C(8)}$ (65°). Since coupling constants are generally maximized at dihedral angles of about 180°, and minimized for angles between 65 and 90°,[18] we assign the C(4) resonance as the one with $A = 0.168$ MHz and the C(8) resonance as the one shifting only slightly with temperature (Table IV and Figure 2).

The electron–nucleus hyperfine coupling constants determined for various carbon nuclei allow us to draw some inferences about the nature of the superexchange pathway in copper(II) *n*-butyrate. We surveyed the literature for solution-state NMR studies of paramagnetic systems from which conclusions about electronic delocalization onto alkyl chains were drawn. Remarkable similarity was found between the trends in sign and relative magnitude of our calculated A values (Table IV) and those observed for alkylamines[19] and quinuclidine[20] coordinated to nickel(II) acetylacetonate. Reasoning by analogy to those studies suggests the following interpretation of the hyperfine coupling constants in copper(II) *n*-butyrate. The decrease in (positive) A moving from C(2) (or C(6)) to C(4) (or C(8)) is explained by invoking σ-delocalization of unpaired electron density onto these carbon nuclei, while the negative A value for C(1) (or C(5)) (which is approximately half the magnitude of A calculated for the adjacent methylene carbon nucleus) is consistent with electronic delocalization via spin polarization by unpaired electron density in lone-pair orbitals on the carboxylate oxygen atoms.

This latter result supports recent nonempirical valence-bond calculations which concluded that the oxygen lone-pair orbitals were the major contributors to the superexchange pathway for copper(II) carboxylates.[21] Also, the observation of σ-delocalized electron density on C(2) through C(4) and C(6) through C(8) suggests that future, more complete descriptions of the antiferromagnetic couplings in such compounds should include mechanisms for delocalization onto σ orbitals along the alkyl chain.

Preliminary experiments with several other anhydrous copper(II) carboxylates are yielding results consistent with those for the title compound, suggesting that solid-state NMR methods will have some general utility in the study of this important class of exchange-coupled transition-metal systems, including compounds that cannot be obtained as single crystals.

Acknowledgment. This work was supported by the National Science Foundation (Grant CHE-8700667) and the Robert A. Welch Foundation (Grant A-1003). We thank Joe Reibenspies for his help in determining the crystal structure.

Supplementary Material Available: Table SI, detailing the structural determination, and Tables SII and SIII, listing thermal parameters and calculated H atom coordinates (3 pages); a listing of calculated and observed structure factors (8 pages). Ordering information is given on any current masthead page.

(18) (a) Schwarcz, J. A.; Perlin, A. S. *Can. J. Chem.* **1972**, *50*, 3667. (b) Marshall, J. L.; Miller, D. E. *J. Am. Chem. Soc.* **1973**, *95*, 8305.
(19) Quaegebeur, J. P.; Chachaty, C.; Yasukawa, T. *Mol. Phys.* **1979**, *37*, 409.
(20) Morishima, I.; Okada, K.; Yonezawa, T.; Goto, K. *J. Chem. Soc., Chem. Commun.* **1970**, 1535.
(21) Harcourt, R. D.; Skrezenek, F. L.; Maclagan, G. A. R. *J. Am. Chem. Soc.* **1986**, *108*, 5403.